

# FACE STABILITY OF SHALLOW CIRCULAR TUNNELS DRIVEN UNDER THE WATER TABLE: A NUMERICAL ANALYSIS

P. DE BUHAN\*, A. CUVILLIER, L. DORMIEUX AND S. MAGHOUS

*Laboratoire de Mécanique des Solides (URA 317), ENPC-CERCSO, 6 et 8 av. Blaise Pascal, Cité Descartes,  
Champs-sur-Marne, 77455 Marne-la-Vallée Cedex 2, France*

## SUMMARY

The stability analysis of a tunnel excavated in a water-saturated frictional soil is investigated in the light of a failure design approach. The soil strength properties being classically formulated in terms of effective stresses, it is first shown how the effect of seepage flow generated by the excavation process, may be accounted for in such an analysis by means of driving body forces derived from the gradient of an excess pore pressures distribution. The latter is obtained as the solution of a hydraulic boundary value problem, in which both water table evolution and soil deformability can be neglected. A variational formulation of this hydraulic problem in terms of filtration velocities is then presented, leading through appropriate numerical treatment, to a search for the minimum without constraints of a quadratic functional (hybrid formulation), which is formulated by a finite element method. Some numerical examples are given, which provide ample evidence of the crucial role played by seepage forces in the tunnel face stability, since the factor of stability may be divided by as much as three. The influence of such parameters as the tunnel relative depth or soil anisotropic permeability is finally discussed, thus offering a first illustration of the various capabilities of this numerical tool. Copyright © 1999 John Wiley & Sons, Ltd.

## 1. INTRODUCTION

The stability of the tunnel face is of paramount importance, particularly in the design of tunnels driven at shallow depths. In the case of purely cohesive grounds, several contributions have been devoted to this subject since the early paper by Broms and Bennermark,<sup>1</sup> which was based on laboratory tests and field observations. A more theoretical approach based on limit analysis was presented by Davis *et al.*,<sup>2</sup> which derived a stability criterion accounting for the effect of tunnel depth. Their results were supported by centrifuge tests.<sup>3</sup>

Less is known about the face stability of tunnels driven in cohesive-frictional grounds. Within the framework of limit analysis, some lower bound solutions were presented by Muelhaus<sup>4</sup> and Leca and Panet,<sup>5</sup> whereas Leca and Dormieux<sup>6</sup> derived an upper bound solution. However, the effect of pore water was not considered in these papers. The aim of the present contribution is to incorporate this effect in the face stability analysis.

When the water table is above the tunnel, seepage flow takes place in the direction of the face and becomes an additional factor of instability. Indeed, the seepage forces prove to be driving

\* Correspondence to: P. de Buhan, Laboratoire de Mécanique des Solides (URA 317), ENPC-CERCSO, 6 et 8 av. Blaise Pascal, Cité Descartes, Champs-sur-Marne, 77455 Marne-la-Vallée Cedex 2, France

forces in any failure mechanism emerging at the tunnel face. The stability analysis which is proposed herein for the face of the tunnel is based on an extension of the simple failure mechanism involving a solid conical block introduced by Leca and Dormieux.<sup>6</sup>

The present contribution is divided into five main sections. It is first shown in Section 2 that, since the soil failure criterion is classically expressed as a function of the effective stress, the stability analysis of the tunnel face subject to water seepage due to the excavation process, involves a field of body forces calculated as the opposite of the gradient of the excess pore pressure distribution. It is then proved in Section 3 that, provided certain conditions be fulfilled, the latter distribution may be calculated as the solution of a simplified hydraulic problem in which the water table may be considered as fixed, while the soil deformations are neglected. Unlike the usual methods employed for solving the hydraulic problem, an original variational formulation of the problem in terms of filtration velocities is proposed in Section 4, and several possible numerical treatments are presented in Section 5. The paper ends with the implementation of one of these numerical methods (the so-called 'hybrid formulation') on an illustrative example (Section 6), where the seepage forces numerically determined through a finite element method are incorporated into the stability analysis.

## 2. PRINCIPLE OF THE STABILITY ANALYSIS

Let us consider a fixed frame  $Ox_1x_2x_3$  where  $Ox_1$  is the tunnel axis and  $Ox_2$  is the upward vertical direction, as well as a moving frame  $O'X_1X_2X_3$  attached to the tunnel face. The geometry is idealized as shown in Figure 1 by considering that the tunnel is a rigid impervious circular cylinder of diameter  $D$  driven under a depth of cover  $C$ .  $H_w$  denotes the height of the undisturbed water table with respect to the tunnel axis. The strength properties are assumed to be uniform around the tunnel: the soil is modelled as a Mohr–Coulomb material, characterized by its cohesion  $c$  and friction angle  $\phi$ . In order to focus this study on the role of pore water and to simplify the comparison with the dry case, we shall assume that gravity is the unique external force to be considered in addition to the seepage forces. The soil unit weight and the water unit weight are denoted by  $\gamma$  and  $\gamma_w$ , respectively.

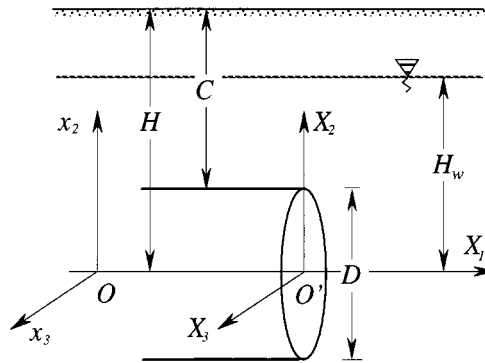
Consider any volume of soil denoted by  $\Omega$ . It is subjected to its weight as well as to the distribution of surface forces  $\mathbf{T} = \boldsymbol{\sigma} \cdot \mathbf{n}$  on its boundary  $\partial\Omega$ , where  $\boldsymbol{\sigma}$  is the total stress tensor and  $\mathbf{n}$  is the outer unit vector normal to  $\partial\Omega$ . The overall equilibrium of  $\Omega$  thus requires that

$$\int_{\partial\Omega} \mathbf{T} \, dS + \int_{\Omega} -\gamma \mathbf{e}_2 \, d\Omega = 0 \quad (1)$$

Let us now introduce the pore pressure  $p$ , the effective stress tensor  $\boldsymbol{\sigma}' = \boldsymbol{\sigma} + p\mathbf{1}$  (convention of positive tensile stress is adopted throughout the text), the corresponding effective stress vector  $\mathbf{T}' = \boldsymbol{\sigma}' \cdot \mathbf{n}$  and the excess pore pressure defined as  $u = p + \gamma_w(x_2 - H_w)$ . Using the divergence theorem, the momentum balance equation (1) can now be written in the form

$$\int_{\partial\Omega} \mathbf{T}' \, dS + \int_{\Omega} -\gamma' \mathbf{e}_2 \, d\Omega + \int_{\Omega} -\mathbf{grad} \, u \, d\Omega = 0 \quad (2)$$

where  $\gamma' = \gamma - \gamma_w$  is the buoyant weight. Equation (2) expresses the overall equilibrium of  $\Omega$  when subjected to its weight minus the buoyancy force, to the distribution of effective stress vectors  $\mathbf{T}'$



on its boundary, and to the seepage body forces equal to  $-\mathbf{grad} u$ . A necessary condition for the tunnel to be safe is that the overall equilibrium of any domain, expressed in terms of total stresses by (1), or in terms of effective stresses by (2), can be ensured under the strength condition  $f(\mathbf{T}') \leq 0$  corresponding to the Mohr–Coulomb criterion.  $\sigma'_n$  and  $\tau$  denoting the effective normal and tangential stress components on any facet of  $\partial\Omega$ , the strength condition is written as

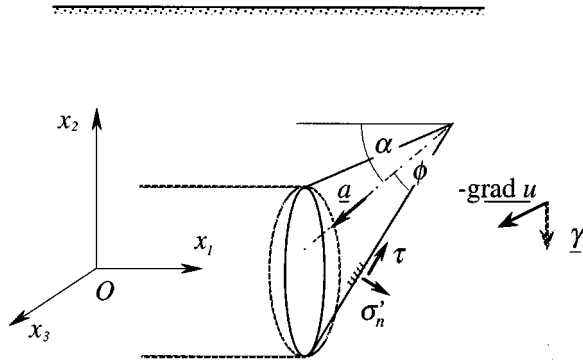


Figure 2. Equilibrium of a conical volume of soil subject to the combined effect of gravity and seepage forces

where  $\mathcal{S}(\alpha)$  is the area of the cone boundary. Equation (6) is a necessary condition of face stability to be satisfied for any conical block of the class defined previously, i.e. for any value of angle  $\alpha$ . This stability condition yields an upper bound for the sum of the seepage force and the gravity force acting on the cone, projected onto the cone axis. This upper bound depends on the cohesion and friction angle of the soil.

In order to derive quantitative stability conditions in a given practical situation, the field  $-\text{grad } u$  of seepage forces must first be determined. Thus, the stability analysis is to be coupled with the hydraulic problem which is now considered.

*Comments:* (a) It is to be emphasized that the above reasoning carried out on the conical volume of soil, does not involve any kind of 'kinematics'. Condition (6) simply expresses the necessary compatibility between equilibrium and strength requirements, with absolutely no reference to any plastic flow rule of the constituent soil. One should refer to Salençon<sup>7</sup> for a detailed discussion of this point.

(b) The present approach may easily be extended to more complex situations than that selected in this paper for illustrative purposes: presence of a supporting pressure applied to the facing, reinforcement of the soil mass by fibreglass bolts placed ahead of the facing, etc.

### 3. THE HYDRAULIC PROBLEM

Denoting by  $\mathbf{v}^f(\mathbf{x}, t)$  and  $\mathbf{v}^s(\mathbf{x}, t)$  the velocities of the fluid and skeleton particles located at the same point  $\mathbf{x}$ , the filtration velocity  $\mathbf{v}$  is defined as  $n(\mathbf{v}^f - \mathbf{v}^s)$ , where  $n$  is the soil porosity.

One major difficulty of the hydraulic problem lies in the fact that the boundary conditions are written on moving surfaces. More precisely, the value of the pore pressure  $p$  is prescribed equal to 0 on the tunnel face whose velocity is denoted by  $V$  and on the water table the position of which at time  $t$  may be described by an equation of the form  $f(x_1, x_2, x_3, t) = x_2 - h(x_1, x_3, t) = 0$ .  $h(x_1, x_3, t)$  represents the local value of hydraulic head (see Figure 3). In addition, condition  $\mathbf{v} \cdot \mathbf{n} = 0$  in which  $\mathbf{n}$  refers to the unit normal vector to the tunnel wall expresses that this surface is impervious.

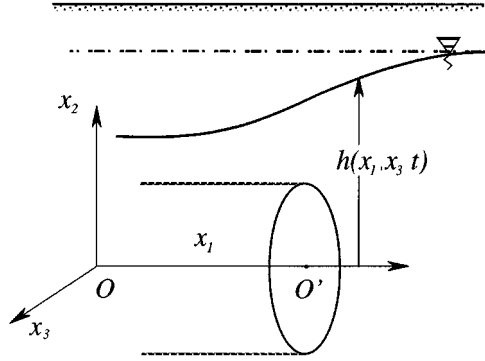


Figure 3. Evolution of the water table due to the excavation process

### 3.1. Evolution of the water table

We first consider the evolution of the water table. Expressing that it is a fluid material surface gives

$$\dot{f} = \frac{\partial f}{\partial t} + \frac{\partial f}{\partial x_i} \dot{x}_i = \frac{\partial f}{\partial t} + \frac{\partial f}{\partial x_i} v_i^f = 0 \quad (7)$$

where  $(\dot{\cdot})$  denotes the time derivative when following a fluid particle. Let us now write Darcy's law in the form

$$v_i = - \frac{k_{ij}}{\gamma_w} \frac{\partial u}{\partial x_j} \quad (8)$$

where  $\mathbf{k}$  is the permeability tensor (which has the dimension of a velocity). For the sake of simplicity, we assume in the following that  $\mathbf{k}$  is an isotropic tensor, so that  $\mathbf{k} = k\mathbf{1}$ . Besides, we neglect the velocity of the skeleton particle with respect to the velocity of the fluid, which writes  $\mathbf{v} \cong n\mathbf{v}^f$ . Combining (7) and (8), one obtains

$$\frac{\partial h}{\partial t} = \frac{k}{n\gamma_w} \left( \frac{\partial u}{\partial x_1} \frac{\partial h}{\partial x_1} + \frac{\partial u}{\partial x_3} \frac{\partial h}{\partial x_3} - \frac{\partial u}{\partial x_2} \right) \quad (9)$$

We shall not try to solve (9), the interest of which is to reveal the characteristic time  $T$  for the evolution of the water table, as well as the characteristic velocity  $V_{wt} = H_w/T$  of the water table. In order to determine  $T$  and  $V_{wt}$ , (9) has to be written in a non-dimensional form. We therefore introduce the following non-dimensional hydraulic head, excess pore pressure, time and space co-ordinates:

$$\bar{h} = \frac{h}{H_w}, \quad \bar{u} = \frac{u}{\gamma_w H_w}, \quad \bar{t} = \frac{t}{T}, \quad \bar{x}_i = \frac{x_i}{H_w} \quad (10)$$

With these notations, (9) becomes

$$\frac{\partial \bar{h}}{\partial \bar{t}} = \frac{kT}{nH_w} \left( \frac{\partial \bar{u}}{\partial \bar{x}_1} \frac{\partial \bar{h}}{\partial \bar{x}_1} + \frac{\partial \bar{u}}{\partial \bar{x}_3} \frac{\partial \bar{h}}{\partial \bar{x}_3} - \frac{\partial \bar{u}}{\partial \bar{x}_2} \right) \quad (11)$$

$T = nH_w/k$  thus appears as the characteristic time  $T$  for the evolution of the water table. The associated characteristic velocity is  $V_{wt} = k/n$ . This result means that the disturbance of the water table induced by the excavation process (with respect to the original horizontal situation) is controlled by the ratio  $V/V_{wt} = nV/k$ . The higher  $V/V_{wt}$ , the smaller the disturbance.

In the following, we assume that this ratio is high enough so that the evolution of the water table can be neglected. As far as the determination of seepage forces and the stability analysis of the tunnel face are concerned, such an approximation proves to be conservative. However, for smaller values of  $V/V_{wt}$ , the influence of tunnel excavation on the water table evolution should be taken into account.<sup>8</sup>

### 3.2. Displacement of the tunnel face

We now deal with the fact that the tunnel face is a moving boundary with constant velocity  $V$  with respect to the  $Ox_1$ -axis. Let us denote by  $x_{i0}$  the initial co-ordinates of a given skeleton particle. Under steady-state conditions, the displacement vectors  $\xi$  of point  $M_1(x_{i0})$  at time  $t$  and point  $M_2(x_{10} + V\tau, x_{20}, x_{30})$  at time  $t + \tau$  are equal:

$$\xi(x_{10}, x_{20}, x_{30}, t) = \xi(x_{10} + V\tau, x_{20}, x_{30}, t + \tau) \quad (12)$$

In other words, the displacement vector and, consequently, the strain tensor  $\varepsilon$  depend on time  $t$  and space co-ordinate  $x_{10}$  through the difference  $x_{10} - Vt$ . In particular, the partial derivatives of any strain component  $\varepsilon_{ij}$  with respect to  $t$  and  $x_{10}$  satisfy

$$\dot{\varepsilon}_{ij} = \frac{\partial \varepsilon_{ij}}{\partial t} = -V \frac{\partial \varepsilon_{ij}}{\partial x_{10}} \quad (13)$$

In order to simplify the reasoning, we assume that the soil permeability is isotropic and homogeneous. Moreover, we consider, as usual in soil mechanics, that the solid material which constitutes the skeleton as well as the fluid are incompressible, so that the diffusion equation can be written as

$$\dot{\varepsilon}_{ii} = \frac{k}{\gamma_w} \sum_i \frac{\partial^2 u}{\partial x_i^2} = \frac{k}{\gamma_w} \Delta_x u \quad (14)$$

The generation of an excess pore pressure field  $u$  results from the difference in hydraulic head between the tunnel face and the water table, as well as from the volume strain of the skeleton. As a matter of fact, (14) recalls that the determination of the excess pore pressure  $u$  and of the skeleton strain are coupled. In order to examine under which conditions this coupling can be neglected, i.e.  $\Delta_x u = 0$ , we now write (14) in a non-dimensional form. As far as the effect of the excavation on deformation is concerned, the appropriate characteristic length is the tunnel diameter  $D$ , whereas the height  $H_w$  is the characteristic length of the seepage associated with the difference in hydraulic head between the tunnel face and the water table. Focusing on the situation of shallow tunnels for which  $D$  and  $H_w$  are of the same order of magnitude, we again introduce as in (10) the non-dimensional co-ordinates  $\bar{x}_i = x_i/H_w$ .

Let  $U$  be the order of magnitude of the excess pore pressure  $u$ . Then, the order of magnitude of the skeleton strain is  $\varepsilon = U/E_0$ , where  $E_0$  is the drained Young's modulus. The characteristic time of consolidation is  $T_c = H_w^2/(kE_0/\gamma_w)$  and the associated characteristic velocity is  $V_c = H_w/T_c$ .

We introduce the normalized excess pore pressure  $\bar{u}$  and strain  $\bar{\varepsilon}_{ij}$  defined as

$$\bar{u} = \frac{u}{U}, \quad \bar{\varepsilon}_{ij} = \frac{\varepsilon_{ij}}{\varepsilon} \quad (15)$$

With these notations, combining (14) with (13) now yields

$$-\frac{V}{V_c} \frac{\partial \bar{\varepsilon}_{ii}}{\partial \bar{x}_{10}} = \Delta_x \bar{u} \quad (16)$$

In the following, we shall assume that  $V/V_c \ll 1$ . According to (16), this implies that the skeleton volume strain can be neglected as far as the determination of the excess pore pressure is concerned, so that (14) can be replaced by  $\Delta_x u = 0$ . From a physical point of view, this means that the excess pore pressure induced by the excavation can dissipate if the face velocity is slow enough. In this case, the excess pore pressure entirely results from the difference in hydraulic head between the tunnel face and the water table.

### 3.3 A simplified framework for the resolution of the hydraulic problem

Let us summarize the results obtained in the two previous sections. If  $V/V_{wt} \gg 1$  and  $V/V_c \ll 1$ , we have concluded that  $u$  can be estimated by the pressure corresponding to the situation of a fixed tunnel face ( $V = 0$ ) in a undeformable soil, the water table being maintained at the plane  $x_2 = H_w$ . Denoting the  $X_i$  the co-ordinates in a frame attached to the tunnel face (Figure 1), the equations of the differential problem to be satisfied by  $u$  are

$$X_2 \leq H_w, \quad \Delta_x u = \sum_i \frac{\partial^2 u}{\partial X_i^2} = 0 \quad (17)$$

$$(\sqrt{X_2^2 + X_3^2} = D/2; \quad X_1 \leq 0), \quad \frac{\partial p}{\partial n} = 0 \quad (18)$$

$$(\sqrt{X_2^2 + X_3^2} \leq D/2, \quad X_1 = 0) \text{ and } (X_2 = H_w), \quad p = 0 \quad (19)$$

It is recalled that the pressure  $p$  and the excess pore pressure  $u$  are related by  $u = p + \gamma_w (X_2 - H_w)$ . In the framework of these assumptions, the resolution of the hydraulic problem and, in particular, the determination of the seepage forces  $-\mathbf{grad} u$  which are necessary for the stability analysis can be done without considering the displacements of the boundaries (water table and tunnel face) nor the coupling with the skeleton deformation.

In practice, the velocity of the tunnel face is of the order of  $1 \text{ m h}^{-1}$ .  $V_{wt}$  and  $V_c$  being both proportional to the permeability, conditions  $V/V_{wt} \gg 1$  and  $V/V_c \ll 1$  will be most restrictive for high and low permeabilities, respectively. Even for a sand with a typical permeability of  $10^{-5} \text{ m s}^{-1}$  and a porosity of 0.3, we obtain a characteristic velocity  $V_{wt}$  of the table of about  $12 \text{ cm h}^{-1}$ , so that the condition  $V/V_{wt} \gg 1$  is still reasonably satisfied. Besides, with a drained constrained modulus of the order of  $10^2 \text{ MPa}$ , the characteristic velocity of consolidation  $V_c$  for a sand is of the order of  $36 \text{ m h}^{-1}$  which fulfills condition  $V_c \gg V$ . On the contrary, in the case of a clay, with drained constrained modulus of the order of  $10 \text{ MPa}$  and a permeability of

$10^{-9} \text{ m s}^{-1}$ ,  $V_c$  is of the order of  $3.6 \text{ cm h}^{-1}$ . Consequently, the simplified framework based on the two assumptions  $V_{wt} \ll V \ll V_c$  which is adopted in the following is suitable for sands but not for clays. For the latter, observing that  $V_c \ll V$ , we conclude that the excess pore pressure induced by the excavation cannot dissipate, so that an undrained stability analysis is justified (see Reference 2).

#### 4. RESOLUTION OF THE SIMPLIFIED HYDRAULIC PROBLEM: THEORETICAL ASPECTS

Under the conditions  $V/V_{wt} \gg 1$  and  $V/V_c \ll 1$ , it has been shown in the previous section that the excess pore pressure distribution  $u$  can be approximated by the solution of (17) together with the boundary conditions (18) and (19). More generally, we shall now consider the following uncoupled hydraulic problem (steady state flow, no skeleton volume strain):

Fine  $u$  such that

$$\text{div}(-\mathbf{k} \cdot \mathbf{grad} u) = 0 \quad \text{in } \Omega \quad (20)$$

$$\partial\Omega_u: u = u^d \quad (21)$$

$$\partial\Omega_v: \frac{1}{\gamma_w} \mathbf{n} \cdot \mathbf{k}(-\mathbf{grad} u) = v^d \quad (22)$$

where  $\mathbf{k}$  is a given permeability tensor field,  $u^d$  (resp.  $v^d$ ) is the prescribed value of the excess pore pressure (resp. the normal component of the fluid velocity) on the boundary  $\partial\Omega_u$  (resp.  $\partial\Omega_v$ ) and  $\mathbf{n}$  is the outer unit normal to  $\partial\Omega_v$ .

This is a classical differential problem which is usually numerically solved with respect to the unknown  $u$  by the finite element method. This approach is based on a well-known variational theorem which states that the solution  $u$  achieves the minimum of the following functional:

$$J(u') = \frac{1}{2\gamma_w} \int_{\Omega} \mathbf{grad} u' \cdot \mathbf{k} \cdot \mathbf{grad} u' d\Omega + \int_{\partial\Omega_v} u' v^d dS \quad (23)$$

over the set  $\mathcal{P}$  of 'admissible' pressure fields  $u'$  defined as follows:

$$\mathcal{P} = \{u', u' \text{ continuous and piecewise differentiable, } u' = u^d \text{ on } \partial\Omega_u\} \quad (24)$$

However, we have seen that the excess pore pressure is involved in the stability analysis through its gradient  $\mathbf{grad} u$  (see (6)). This is why it seems more appropriate to develop a method of resolution of (20)–(22) with respect to the filtration velocity  $-(1/\gamma_w)\mathbf{k} \cdot \mathbf{grad} u$ . The aim of this section is to determine the corresponding variational approach. We therefore introduce the set  $\mathcal{V}$  of 'admissible' filtration velocity fields  $\mathbf{v}'$  subject to the following conditions:

- (i)  $\mathbf{v}'$  is piecewise continuous and differentiable;
- (ii)  $\text{div} \mathbf{v}' = 0$ ;
- (iii) the normal component  $\mathbf{v}' \cdot \mathbf{n}$  of  $\mathbf{v}'$  is continuous across possible jump surfaces  $\Sigma$  of unit normal  $\mathbf{n}$ ;
- (iv)  $\mathbf{v}' \cdot \mathbf{n} = v^d$  on  $\partial\Omega_v$ , where  $\mathbf{n}$  is the outer unit normal to  $\partial\Omega_v$ .



Conditions (ii) and (iii) actually express the requirement of fluid mass conservation. Let us now define on  $\mathcal{V}$  the following functional:

$$J^*(\mathbf{v}') = \frac{\gamma_w}{2} \int_{\Omega} \mathbf{v}' \cdot \mathbf{k}^{-1} \cdot \mathbf{v}' d\Omega + \int_{\partial\Omega_u} u^d \mathbf{v}' \cdot \mathbf{n} dS \quad (25)$$

The theorem constituting the theoretical basis of the numerical method which will be presented in the next section states that the solution  $\mathbf{v}$  of the differential problem (20)–(22) achieves the minimum of the functional  $J^*$  over  $\mathcal{V}$ .

In order to prove this result, let us write any element  $\mathbf{v}'$  of  $\mathcal{V}$  in the form  $\mathbf{v}' = \mathbf{v} + \delta\mathbf{v}$  obviously satisfies (i)–(iii), while (iv) is replaced by

$$\delta\mathbf{v} \cdot \mathbf{n} = 0 \quad \text{on } \Omega_v \quad (26)$$

Applying the definition (25) of functional  $J^*$ , one obtains

$$J^*(\mathbf{v} + \delta\mathbf{v}) = J^*(\mathbf{v}) + \frac{\gamma_w}{2} \int_{\Omega} \delta\mathbf{v} \cdot \mathbf{k}^{-1} \cdot \delta\mathbf{v} d\Omega + \gamma_w \int_{\Omega} \delta\mathbf{v} \cdot \mathbf{k}^{-1} \cdot \mathbf{v} d\Omega + \int_{\partial\Omega_u} u^d \delta\mathbf{v} \cdot \mathbf{n} dS \quad (27)$$

Recalling that the excess pore pressure  $u$  and the fluid velocity  $\mathbf{v}$  which are solutions of the problem are related by Darcy's law (8), an integration by parts of the second integral of (27) yields

$$\gamma_w \int_{\Omega} \delta\mathbf{v} \cdot \mathbf{k}^{-1} \cdot \mathbf{v} d\Omega = \int_{\Omega} u \operatorname{div} \delta\mathbf{v} d\Omega - \int_{\partial\Omega} u \delta\mathbf{v} \cdot \mathbf{n} dS \quad (28)$$

Using the fact that  $\operatorname{div} \delta\mathbf{v} = 0$  together with (26), (28) can be written as

$$\gamma_w \int_{\Omega} \delta\mathbf{v} \cdot \mathbf{k}^{-1} \cdot \mathbf{v} d\Omega = - \int_{\partial\Omega_u} u^d \delta\mathbf{v} \cdot \mathbf{n} dS \quad (29)$$

Combining (27) and (29), one obtains

$$(\forall \mathbf{v}' \in \mathcal{V}) J^*(\mathbf{v}') = J^*(\mathbf{v}) + \frac{\gamma_w}{2} \int_{\Omega} (\mathbf{v}' - \mathbf{v}) \cdot \mathbf{k}^{-1} \cdot (\mathbf{v}' - \mathbf{v}) d\Omega \quad (30)$$

The proof of the announced variational theorem finally results from the fact that  $\mathbf{k}$  is a definite positive tensor.

## 5. NUMERICAL APPROACH TO THE FILTRATION VELOCITY FORMULATION

Due to its mathematical structure, the above variational formulation of the uncoupled hydraulic problem is amenable to a numerical treatment. Two different methods will now be presented. Although they both rely on finite element discretization techniques, each of them has given rise to original developments.

### 5.1. Hybrid formulation

Considering, for instance, a given discretization of the geometric domain  $\Omega$  into finite elements, the minimization of functional  $J^*(\mathbf{v}')$  is carried out by generating discretized filtration velocity

fields, the restriction of which to any individual element being expressed as a polynomial function of space co-ordinates. Unfortunately, due to condition (ii) which must be satisfied within any such element, and to condition (iii) as well relating to velocity jumps across separation lines between adjacent elements, the direct implementation of this method proves quite difficult.

A possible way of overcoming such a difficulty consists in relaxing the above-mentioned kinematic constraints by the introduction of Lagrange multipliers. Such a procedure refers to the so-called hybrid methods.<sup>9</sup>

Let  $\Sigma$  denote a given set of surfaces dividing  $\Omega$  into a finite number of subdomains. The following functional is then defined:

$$F(\mathbf{v}', \lambda, \mu) = J^*(\mathbf{v}') - \int_{\Omega} \lambda \operatorname{div} \mathbf{v}' d\Omega - \int_{\Sigma} \mu [\llbracket \mathbf{v}' \rrbracket] \cdot \mathbf{n} dS + \int_{\partial\Omega_p} \mu (\mathbf{v}' \cdot \mathbf{n} - v^d) dS \quad (31)$$

where  $\mathbf{v}'$  represents any piecewise differentiable trial vector field defined on  $\Omega$ , which is no more subject to the divergence-free condition (ii), as well as to conditions (iii) on  $\Sigma$  ( $[\llbracket \mathbf{v}' \rrbracket]$  is the jump of  $\mathbf{v}'$  across  $\Sigma$ ) and (iv) on  $\partial\Omega_p$ , respectively.  $\lambda$  and  $\mu$  are the Lagrange multipliers associated with those constraints.

It can be proved (see, for instance, References 10 and 11) that if  $(\mathbf{v}', \lambda, \mu)$  realizes the stationarity of functional  $F$ , then  $\mathbf{v}' = \mathbf{v}$ , where  $J^*(\mathbf{v}) = \min\{J^*(\mathbf{v}'), \mathbf{v}' \in \mathcal{V}\}$ , while  $\lambda$  (resp.  $\mu$ ) is identical with the excess pore pressure solution  $u$  in each subdomain of  $\Omega$  (resp. on  $\Sigma$  and  $\partial\Omega_p$ ). For the sake of simplicity,  $\mathbf{v} \cdot \mathbf{n} = v^d = 0$  (impervious boundary) will now be considered.

*5.1.1. Numerical discretization.* The domain  $\Omega$  under consideration is first discretized into a mesh of finite elements  $K$ , so that  $\Sigma$  is formed by the set of surfaces separating adjacent elements. Let  $P_k$  denote the set of scalar or vector fields whose components are expressed as polynomial functions of degree  $k$  with respect to space co-ordinates. It may be shown that selecting

$$\mathbf{v}'_{|K} \in P_k, \quad \lambda_{|K} \in P_{k-1}, \quad \mu_{|K \cap K'} \in P_k \quad \text{and} \quad \mu_{|\partial\Omega_u} = 0 \quad (32)$$

the triple  $(\mathbf{v}', \lambda, \mu)$  making  $F$  stationary is such that  $\mathbf{v}'$  rigorously satisfies conditions (i)–(iv). More specifically, following a usual approach,  $\mathbf{v}'$ ,  $\lambda$  and  $\mu$  may be written as

$$\mathbf{v}'_{|K} = \mathbf{N}_K \cdot \mathbf{V}_K, \quad \lambda_{|K} = \mathbf{M}_K^T \cdot \boldsymbol{\Lambda}_K, \quad \mu_{|\partial K} = \mathbf{L}_{\partial K}^T \cdot \boldsymbol{\mu}_{\partial K} \quad (33)$$

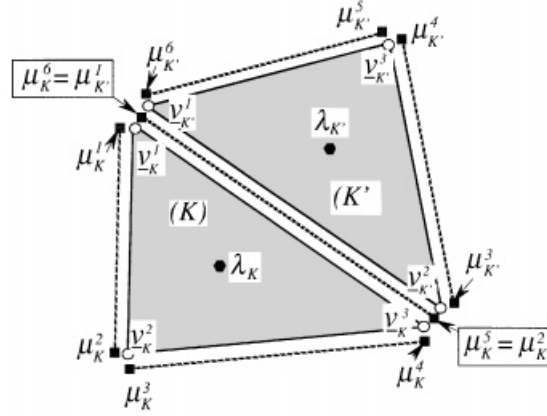
In the latter expressions  $\mathbf{V}_K$  and  $\boldsymbol{\Lambda}_K$  are vectors formed by the nodal values of  $\mathbf{v}'$  and  $\lambda$  of element  $K$ , which are completely independent of those relating to adjacent elements. On the other hand, the components of  $\boldsymbol{\mu}_{\partial K}$  are linked to those of  $\boldsymbol{\mu}_{\partial K'}$  where  $K'$  is adjacent to  $K$ , since they are coincident on the surface separating  $K$  and  $K'$ .  $\mathbf{N}_K$ ,  $\mathbf{M}_K$  and  $\mathbf{L}_{\partial K}$  represent the interpolation functions. By way of example, Figure 4 depicts two adjacent triangular elements (T3) with the corresponding nodal values, associated to a linear interpolation of  $\mathbf{v}'$  ( $k = 1$ ) in the 2-D case.

Since the divergence of  $\mathbf{v}'$  inside each element can be written in the form

$$\operatorname{div} \mathbf{v}'_{|K} = \mathbf{D}^T \cdot \mathbf{V}_K \quad (34)$$

the discretized form of functional  $F$  is

$$F(\mathbf{v}', \lambda, \mu) = \sum_K F_K = \sum_K \frac{1}{2} \mathbf{V}_K^T \cdot \mathbf{r}_K \cdot \mathbf{V}_K - \mathbf{V}_K^T \cdot \mathbf{f}_K - \mathbf{V}_K^T \cdot \mathbf{b}_K \cdot \boldsymbol{\Lambda}_K + \mathbf{V}_K^T \cdot \mathbf{c}_{\partial K} \cdot \boldsymbol{\mu}_{\partial K} \quad (35)$$

Figure 4. Nodal variables attached to two adjacent triangular elements ( $k = 1$ )

with

$$\begin{aligned} \mathbf{r}_K &= \gamma_w \int_K \mathbf{N}^T \cdot \mathbf{k}^{-1} \cdot \mathbf{N} \, d\Omega, \quad \mathbf{f}_K = - \int_{\partial K \cap \partial \Omega_u} u^d \mathbf{N}^T \cdot \mathbf{n} \, dS \\ \mathbf{b}_K &= \int_K \mathbf{D} \cdot \mathbf{M}^T \, d\Omega, \quad \mathbf{c}_{\partial K} = \int_{\partial K} \mathbf{N}^T \cdot \mathbf{n} \cdot \mathbf{L}^T \, dS \end{aligned}$$

*5.1.2. Solving the discretized problem.* Thanks to the specific choice made for the different spaces of trial functions, the number of variables involved in (35) can be considerably reduced. Indeed, since for a given finite element  $K$ , the variables corresponding to  $\mathbf{V}_K$  and  $\mathbf{\Lambda}_K$  do not appear in any other term than  $F_K$ , expressing the stationarity condition with respect to these variables leads to

$$\begin{aligned} \partial F / \partial \mathbf{V}_K &= \partial F_K / \partial \mathbf{V}_K = 0 \\ \partial F / \partial \mathbf{\Lambda}_K &= \partial F_K / \partial \mathbf{\Lambda}_K = 0 \end{aligned} \quad (36)$$

which constitutes a system of linear equations making it possible to calculate  $\mathbf{V}_K$  and  $\mathbf{\Lambda}_K$  as functions of  $\boldsymbol{\mu}_{\partial K}$  only. It follows that (35) can be rewritten in the form

$$F = \sum_K F_K = -\frac{1}{2} \boldsymbol{\mu}^T \cdot \mathbf{R} \cdot \boldsymbol{\mu} + \boldsymbol{\mu}^T \cdot \mathbf{F} + Q \quad (37)$$

where  $\boldsymbol{\mu}$  is the vector formed by all the nodal variables associated with the Lagrange multiplier  $\mu$ . It should be noted that the only trial velocity field  $\mathbf{v}'$  calculated from  $\boldsymbol{\mu}$  through equation (36), which belongs to  $\mathcal{V}$ , that is complies with conditions (i)–(iv), is that corresponding to the vector  $\boldsymbol{\mu}$  minimizing (37). The latter minimization should therefore be carried out carefully, in order to determine the minimum of (37) with the best possible accuracy.

## 5.2. Vector potential approach

This alternative numerical method is derived from that classically introduced in the mechanics of incompressible fluids.<sup>12</sup> While its numerical implementation is straightforward in the

two-dimensional case, its application to three-dimensional problems, such as evaluating the seepage forces around a tunnel face, requires some adaptations. The latter, which will now be briefly presented, may be found in Reference 13 where the method has been applied to the calculation of limit loads of 3D-structures.

It is based on the following property.<sup>12</sup> Any velocity field  $\mathbf{v}'$  satisfying conditions (i)–(iv) is such that there exists a vector field  $\boldsymbol{\Psi}'$  (called ‘vector potential’) everywhere continuous and with piecewise continuous derivatives satisfying

$$\mathbf{v}' = -\mathbf{curl} \boldsymbol{\Psi}' \quad \text{with } \forall \mathbf{x} \in \Omega \quad \boldsymbol{\Psi}'(\mathbf{x}) = \psi'_1(x_1, x_2, x_3)\mathbf{e}_1 + \psi'_2(x_1, x_2, x_3)\mathbf{e}_2 \quad (38)$$

where  $(O, \mathbf{e}_1, \mathbf{e}_2, \mathbf{e}_3)$  is an orthonormal frame. It can be easily verified that  $\text{div } \mathbf{v}' = 0$  outside surfaces  $\Sigma$  where  $\mathbf{grad} \boldsymbol{\Psi}'$  is discontinuous, whereas the jump of  $\mathbf{v}'$  across such surfaces can be written as

$$[[\mathbf{v}']] = \left[ \left[ \frac{\partial \boldsymbol{\Psi}'}{\partial n} \right] \right] \wedge \mathbf{n} \quad (39)$$

where  $\mathbf{n}$  is the unit normal to  $\Sigma$ , which shows that the velocity jump is purely tangential. It is worth noting that  $\boldsymbol{\Psi}'$  is defined up to a gradient of any arbitrary scalar function of co-ordinates  $x_1$  and  $x_2$ .  $\boldsymbol{\Psi}'$  may be uniquely determined by imposing, for instance, that it be equal to zero on any plane normal to  $\mathbf{e}_3$ .

It follows that the initial minimization problem relative to functional  $J^*(\mathbf{v}')$  can be replaced by the following one:

$$\text{Find } \boldsymbol{\Psi} = (\psi_1, \psi_2) \quad \text{such that} \quad \mathcal{Y}^*(\boldsymbol{\Psi}) = \min_{\boldsymbol{\Psi}'} \mathcal{Y}^*(\boldsymbol{\Psi}'), \quad (40)$$

where  $\mathcal{Y}^*(\boldsymbol{\Psi}') = J^*(\mathbf{v}')$ ,  $\boldsymbol{\Psi}'$  being assigned to boundary conditions which are now specified.

Due to the symmetry of the problem with respect to the  $Ox_1x_2$  plane (vertical plane containing the tunnel axis), the geometry domain to be considered for discretization is the water-saturated soil mass enclosed in the parallelepipedic volume bounded by the following planes (Figure 5):

$$\begin{aligned} P_3^0 \text{ (plane of symmetry: } x_3 = 0) \quad \text{and} \quad P_3^- (x_3 = x_3^- < 0); \\ P_1^+ (x_1 = x_1^+ > 0) \quad \text{and} \quad P_1^- (x_1 = x_1^- < 0); \\ P_2^{\text{wt}} \text{ (water table: } x_2 = H_w) \quad \text{and} \quad P_2^- (x_2 = x_2^- < 0) \end{aligned} \quad (41)$$

with the corresponding boundary conditions regarding the vector potential  $\boldsymbol{\Psi}'$ :

$$\psi'_1 = \psi'_2 = 0 \text{ on } P_3^- \quad (42a)$$

$$\mathbf{v}' \cdot \mathbf{n} = -\mathbf{curl} \boldsymbol{\Psi}' \cdot \mathbf{n} = 0 \text{ on } S_{\text{tw}} \text{ (impervious tunnel wall)} \quad (42b)$$

and  $P_3^0$  (symmetry condition)

$$\psi'_2 = 0 \text{ on } P_1^+ \text{ and } P_1^-, \psi'_1 = 0 \text{ on } P_2^- \quad (42c)$$

Conditions (42c) express the fact that  $P_1^\pm$  and  $P_2^-$  are impervious planes, which is a reasonable assumption provided that they are located sufficiently far away from the tunnel face.

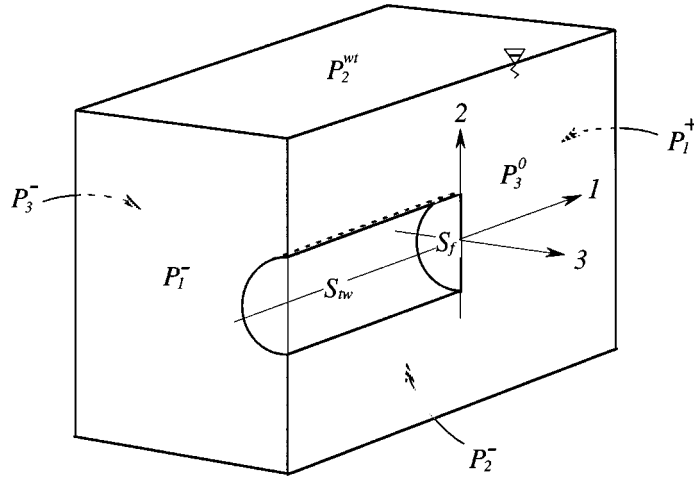


Figure 5. Definition of the geometric domain to be discretized into finite elements

As a consequence of the discretization of the above domain into finite elements, the minimization problem (40) classically reduces to

$$\begin{aligned} &\text{Find } \Psi \text{ minimizing } F = \frac{1}{2} \Psi'^T \cdot \mathbf{R} \cdot \Psi' - \Psi'^T \cdot \mathbf{F} \\ &\text{subject to } \Psi'^T \cdot \mathbf{B} = \mathbf{0} \end{aligned} \quad (43)$$

where  $\Psi'$  is the vector formed by all the nodal values of  $(\psi'_1, \psi'_2)$ , except those assigned to be equal to zero (conditions (42a) and (42c)), and  $\mathbf{B}$  denotes the matrix by means of which boundary conditions (42b) are expressed.

Three different methods may be employed to obtain the solution of (43) numerically. First, by imposing  $\Psi' = \mathbf{0}$  instead of (42b) on  $S_{tw}$  and  $P_3^0$ , thus leading to a problem of minimization without constraints. Its major drawback is to notably reduce the quality of the approximation of  $\mathbf{v}$ , since the space of  $\Psi'$  to be explored in the minimization process is restricted. A second possible way would consist in extracting from condition  $\Psi'^T \cdot \mathbf{B} = \mathbf{0}$  a set of independent nodal variables, so that (43) would again be reduced to a minimization problem without constraints. The feasibility of this second approach relies upon the possibility of extracting those independent variables in a systematic way. Finally, we may also turn to the use of Lagrange multipliers in order to take condition  $\Psi'^T \cdot \mathbf{B} = \mathbf{0}$  into account in the minimization procedure. The main limitation to this third approach is to significantly increase the size of the numerical problem to be handled.

## 6. APPLICATION TO THE TUNNEL STABILITY PROBLEM

In order to illustrate the approach, and more specifically the hybrid formulation, the following example will be considered: horizontal circular tunnel of diameter  $D = 8$  m, driven at a depth equal to  $H = 12$  m (cover  $C = H - D/2 = 8$  m), the water table being coincident with the free

horizontal surface ( $H_w = 12$  m). The soil characteristics are  $\gamma = 18$  kN/m<sup>3</sup>,  $c = 20$  kPa,  $\phi = 30^\circ$ , while its permeability is assumed to be homogeneous, but possibly anisotropic,  $k_h = k_{11} = k_{33}$  and  $k_v = k_{22}$  being the corresponding principle values. It is worth noting that the solution of the hydraulic boundary value problem expressed in terms of excess pore pressure distribution  $u$  depends solely on the ratio  $k_h/k_v$  between the horizontal and vertical soil permeabilities, and not on their individual magnitudes.

The domain to be discretized into tetrahedric elements, with a linear interpolation of the filtration velocity fields (T4 elements), is defined by conditions (41) with  $x_1^-/D = -x_2^-/D = -x_3^-/D = 3$  and  $x_3^+/D = 4$  (Figure 6(a)). The corresponding mesh is made up of 11 238 elements corresponding to 2344 geometric nodes. Making use of the hybrid method described in Section 5.1, it thus leads to 69 288 degrees of freedom corresponding to the interface nodal variables attached to the Lagrange multiplier  $\mu$ . Figure 6(b) displays the associated seepage velocity field in the vicinity of the tunnel face. The computational time necessary for performing the minimization of the quadratic functional defined by (37) on a SUN SPARC 20 workstation amounts to 1 h 17 min, which remains quite reasonable in spite of the relatively high number of degrees of freedom. This good performance may be explained as follows. The number of non-zero terms of the global matrix  $\mathbf{R}$  is much smaller than its total number of components, which is a result of the previous elimination of all nodal variables, apart from those located on the element interfaces. Moreover, the fact that  $\mathbf{R}$  is definite positive, allows the use of a conjugate-gradient algorithm where only the non-zero terms need to be stored at each step of the minimization process.

Considering now the tunnel face stability problem stated in Section 2, in which  $-\mathbf{grad} u$  is acting as a body forces distribution, the necessary condition (6) of the face stability, may be conveniently rewritten as

$$\Gamma(\alpha) = \frac{c \cos \phi \mathcal{S}(\alpha)}{\gamma' \cos \alpha \mathcal{V}(\alpha) + \int_{\mathcal{C}} -\mathbf{a}(\alpha) \cdot \mathbf{grad} u \, d\mathcal{C}} \geq 1 \quad (44)$$

thus introducing a dimensionless factor assessing the stability of the conical volume. For each value of  $\alpha$ , the volume integral is computed numerically by integrating over all elements or subelements of the mesh included in  $\mathcal{C}$ , the following quantity:

$$\mathbf{a}(\alpha) \cdot (\gamma_w \mathbf{k}^{-1} \cdot \mathbf{v}(\boldsymbol{\mu}^*)) \quad (45)$$

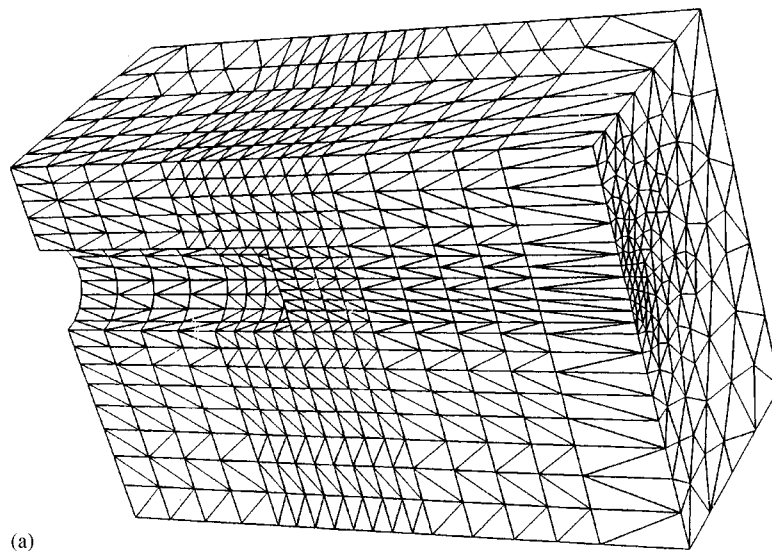
where  $\boldsymbol{\mu}^*$  realizes the minimum of the quadratic functional (37) as explained in Section 5.1,  $\mathbf{v}(\boldsymbol{\mu}^*)$  being the corresponding discretized filtration velocity field.

Varying the inclination  $\alpha$  of the cone axis, makes it then possible to calculate the minimum value of  $\Gamma(\alpha)$ :

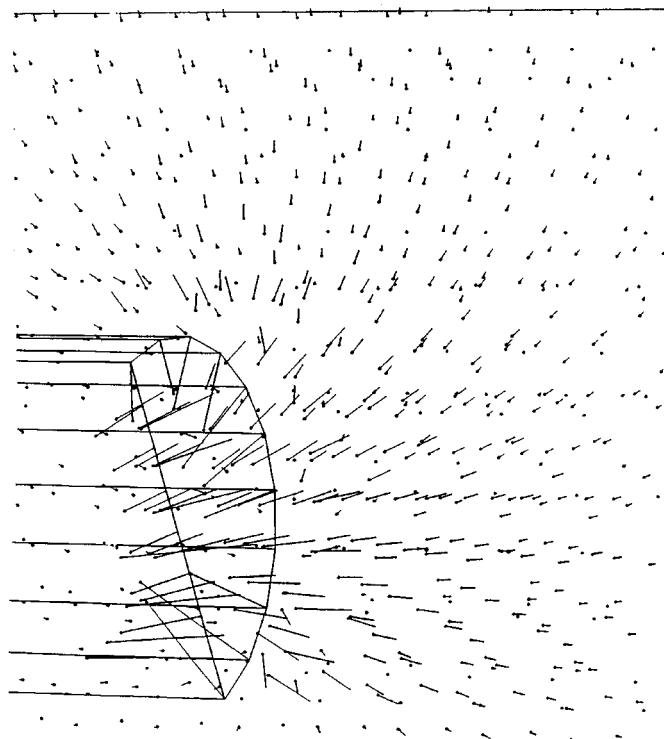
$$\Gamma_{\min} = \min_{\alpha} \Gamma(\alpha) \quad (46)$$

Due to the fact that the minimization procedure involved in (46), which is carried out numerically, is restricted to a particular class of cone-shaped soil volumes, whose equilibrium is checked, the value of  $\Gamma_{\min}$  is to be compared with a coefficient of method, greater than unity, so as to ensure the tunnel face stability with a sufficiently large margin of safety.

Calculations of  $\Gamma(=\Gamma_{\min})$  have first been performed in the case of isotropic permeability ( $k_h = k_v$ ), varying the relative depth of the tunnel defined through the ratio  $C/D$ , with  $H_w = H$ .



(a)



(b)

Figure 6. (a) Finite element mesh used in the hydraulic problem; (b) cross-sectional and side views of the seepage flow around the tunnel face

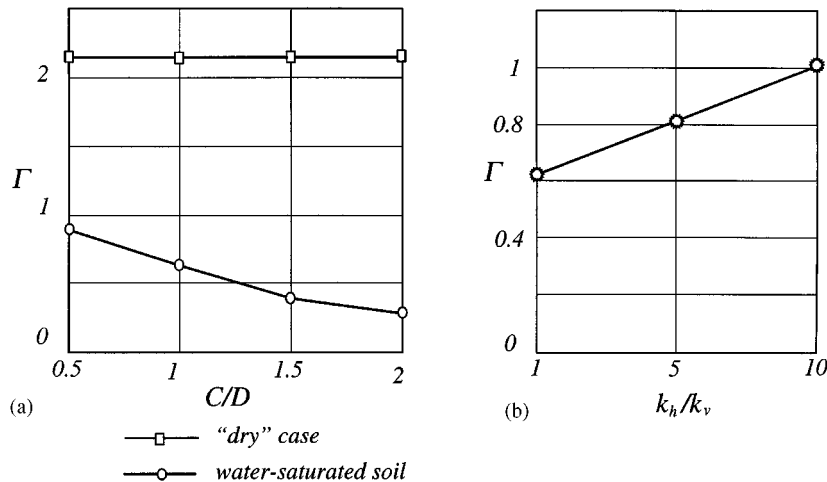


Figure 7. (a) Variations of safety factor as a function of relative depth (isotropic permeability) (b) influence of the permeability anisotropy on the tunnel face stability

The results are reported in Figure 7(a), where the horizontal straight line corresponds to the case of a 'dry' tunnel, while the lower curve is drawn from the numerical results obtained in the presence of water. They suggest the following comments.

It can first be observed that, in the absence of water, the safety factor remains constant equal to 2.12. This is simply due to the fact that, within the range of variations of  $C/D$  (0.5 – 2), the cone-shaped volumes never intersect the above free surface, the position of which having therefore no influence on the result. On the other hand, taking seepage forces into account in the stability analysis of the tunnel face, results in a significant decrease of the stability factor from 0.87 for  $C/D = 0.5$  to 0.27 for  $C/D = 2$ . This is a clear illustration of the predominant role played by seepage flow in the possible collapse of tunnel face.

This first series of calculations has been completed by a parametric study aimed at evaluating the influence of permeability anisotropy. It is quite apparent from Figure 7(b) giving the variations of  $\Gamma$  as a function of  $k_h/k_v = 1, 5, 10$  for  $C/D = 1$ , that a higher horizontal permeability as compared with the vertical one, has a favourable effect on the tunnel face stability.

## 7. CONCLUDING REMARKS

A comprehensive framework has been set up for analysing the stability of geotechnical structures in the presence of seepage flow. It requires being able to evaluate the distribution of excess pore pressures generated by the loading of the structure. In the specific but important situation of shallow tunnels driven in a water-saturated soil, an essential simplification has resulted from the fact that, as far as permeable soils such as sands are considered, water table evolutions as well as soil consolidation may be overlooked in the analysis, leading to a classical hydraulic problem with appropriate boundary conditions. In such a case, an original numerical method, based upon a variational formulation of the problem in terms of filtration velocity fields, has been elaborated, making it possible to calculate the distribution of seepage forces to be incorporated in the



subsequent stability analysis. The possible extension of this approach to other kind of structures in which water flow should be accounted for in the safety analysis, should be considered. It however requires a careful specific analysis, analogous to that developed in the present contribution for shallow tunnels, so as to establish whether the same simplifications are legitimate or not. Such parameters as the ratio between the rate of the loading applied to the structure, and that of the consolidation phenomenon due to the dissipation of excess pore pressures, will undoubtedly play a decisive role in such an analysis.

## REFERENCES

1. B. B. Broms and H. Bennermark, 'Stability of clay at vertical openings', *J. Soil Mech. Found. Div. Am. Soc. Civ. Engrs.*, **93 SM1**, 71–94 (1967).
2. E. H. Davis, M. J. Gunn, R. J. Mair and H. N. Seneviratne, 'The stability of shallow tunnels and underground openings in cohesive material', *Géotechnique*, **30(4)**, 397–416 (1980).
3. A. N. Schofield, 'Cambridge geotechnical centrifuge operations', *Géotechnique*, **30(3)**, 227–288 (1980).
4. H. B. Muelhaus, 'Lower bound solutions for circular tunnels in two or three dimensions', *Rock Mech. Rock Engng.*, **18**, 37–52 (1985).
5. E. Leca and M. Panet, 'Application du calcul à la rupture à la stabilité du front de taille d'un tunnel', *Revue Française de Géotechnique*, **43**, 5–19 (1988).
6. E. Leca and L. Dormieux, 'Upper and lower bound solutions for the face stability of shallow circular tunnels in frictional material', *Géotechnique*, **40(4)**, 581–606 (1990).
7. J. Salençon, 'An introduction to the yield design theory and its application to soil mechanics', *Eur. J. Mech. A/Solids*, **9(5)**, 477–500 (1990).
8. G. Anagnostou, 'The influence of tunnel excavation on the hydraulic head', *Int. J. Numer. Anal. Meth. Geomech.*, **19(10)**, 725–746 (1995).
9. O. C. Zienkiewicz and R. L. Taylor, *The Finite Element Method, Vol. 1.: Basic Formulation and Linear Problems*, 4th edn, McGraw-Hill, 1994.
10. P. A. Raviart and Thomas, 'A mixed finite element method for second order elliptic problems', *Mathematical Aspects of Finite Element Method*, Lecture Notes in Mathematics, Springer, Berlin, 1977.
11. P. A. Raviart, *Les Méthodes D'Éléments Finis En Mécanique des Fluides*, Eyrolles, Paris, 1981.
12. V. Girault and P. A. Raviart, *Finite element Method for Navier–Stokes Equations, Theory and Algorithms*, Springer, Berlin, 1986.
13. S. Maghous and D. Garnier, 'Feasibility of a numerical method for computing the ultimate loads of three dimensional structures', *Mech. Res. Comm.*, **22(3)**, 279–288 (1995).